Ab-Initio Simulation of Diffraction Patterns from Atomistic Models

Ian Robinson

www.starfishprime.co.uk

E-mail: i.robinson@starfishprime.co.uk

Abstract. Lorem ipsum dolor sit amet, consectetuer adipiscing elit. Etiam lobortisfacilisis sem. Nullam nec mi et neque pharetra sollicitudin. Praesent imperdie

1. Introduction

Diffraction techniques provide powerful tools to study how materials order at the atomic level. X-rays were first used to probe microscopic order. These have since been supplemented with electron and neutron diffraction methods. In the specific case of this work the ordered structures produced by Monte-Carlo molecular dynamic simulations can be compared to real world samples by calculating their virtual diffraction patterns for comparison with those from experiment

The study of diffraction patterns from 3-d structures is very well established. Thomas Young famously observed two slit interference of light in ∼1802 concluding that light was a wave rather than a particle as proposed by Newton. Such interference patterns are a natural consequence of the Huygens–Fresnel principle where every point on a wavefront may be assumed to be a source of secondary *wavelets*. 2-d diffraction gratings were well developed by the mid 1800s. The possibility of diffraction from 3-d atomic structures was suggested by Ewald and Laue in 1912 with the first x-ray diffraction pattern produced shortly thereafter.

The terminology used may be somewhat confusing. A *diffraction pattern* is due to the *interference* of *diffracted* waves. However the physical phenomena of interference and diffraction are the same. In physics we tend to use *diffraction pattern* when referring to a few scatterers and *interference pattern* for many. In crystallography the single term *diffraction pattern* is used.

X-rays, electrons and neutrons are used in atomic diffraction studies. Relatively inexpensive and compact equipment is capable of generating x-rays the wavelength of which is of the order of the inter-atomic spacing. X-rays scatter from electrons – thus the scattering power of an atom depends upon the number of electrons it possesses i.e. its atomic number. This hydrogen's low scattering factor means it is difficult to image alongside heavier elements causing problems in determining the structure of organic molecules. Instead thermal neutrons with de-Broglie wavelengths of the order of Angstroms may be used as the neutron scattering factor does not vary simply with Z number and is highest for hydrogen. A suitably bright neutron source may be a nuclear reactor, such as the I.L.L. at Grenoble or a proton synchrotron such as ISIS at the Rutherford-Appleton Laboratory which generates neutrons by spallation from a tungsten target illuminated by GeV energy protons. This equipment is many times larger, more expensive and complex than x-ray diffractometers.

As x-ray, electron and neutron scattering patterns are due to the summing of scattered waves from the target, it is straightforward to simulate this process.

A brief overview of scattering theory is first presented followed by a discussion of how a diffraction pattern may be computed from a simulated sample.

1.1. General Scattering Theory

The kinematic model provides a simple view of scattering. An incident wave-front may be scattered by discontinuities in its path. X-rays scatter from orbital electrons whilst neutrons scatter from atomic nuclei. These scattering centres act as sources of spherical wavefronts (*s-wave* scattering) see fig 1. At some distance wave-fronts from many scatterers interfere thereby creating regions of high and low intensity depending on the phase contributions from each wave. In this simple treatment the scattering is assumed to be elastic i.e. the magnitude of the scattered wave vector is equal to that of the incident. $|\vec{k'}| = |\vec{k}|$. The scattered amplitude A_j arriving at a detector at a distance R_j from the j^{th} atom is given by

$$A_j = A_0 f_j e^{i\vec{K}\cdot\vec{r_j}} \tag{1}$$

Where f_i the *atomic scattering factor* is a measure of the scattering power of the atom. If the distance to the detector is very much greater than the atomic spacing then R_j may be approximated to a constant R see fig 2. In reality a scattered wave is likely to undergo further scattering. In simple models this effect is ignored as it greatly increases computing time.

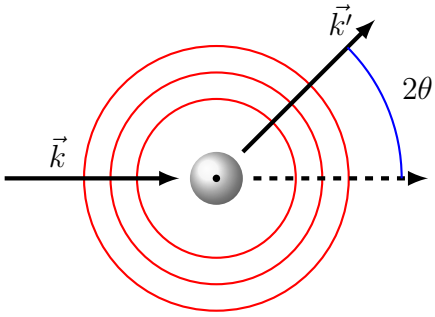

Figure 1: Simple Kinematic Scattering

1.2. The Scattering Vector $\vec{q}$

Consider two atoms i and j, illuminated by a coherent beam of radiation from a source at ∞, of wavelength λ and thus wavevector $|q| = \frac{2\pi}{\lambda}$. The difference between the incident and scattered wave vector is known as the scattering vector where $\vec{k'} = \vec{k} + \vec{q}$ see fig 3.

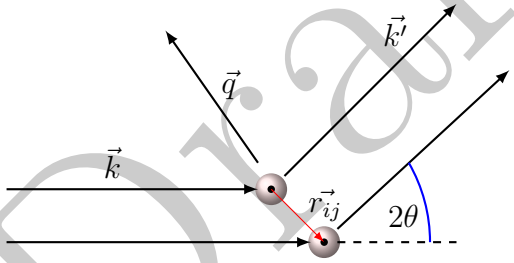

Figure 2: Wave Vectors

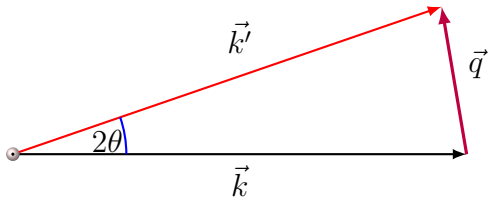

Figure 3: $\vec{k}$ incident, $\vec{k'}$ diffracted and $\vec{q}$ diffraction vectors

Given that $|\vec{k'}| = |\vec{k}|$ and $\angle$ the angle between them

$$|\vec{q}| = 2|\vec{k}| \sin\left(\frac{\vec{k}\angle\vec{k'}}{2}\right) \tag{2}$$

Waves scattered by two atoms i & j scattered as $\vec{q_i}$ and $\vec{q_j}$ will interfere and thus a diffraction pattern will form on the detector.

1.3. Formation of a Diffraction Pattern

We now imagine an ensemble of N identical atoms sitting at 3d positions $\vec{r_i}$ from some arbitrary origin $\vec{r_0}$ with a detector at a distance much greater than the size of the sample see fig 4. We may thus approximate the distance from all points to the detector as a constant and ignore the amplitude-distance terms. The position of each detector pixel may be described by $\vec{k'}$ with respect to the origin of the sample. At some point $\vec{k'}$ on the detector waves scattered from the atoms arrive

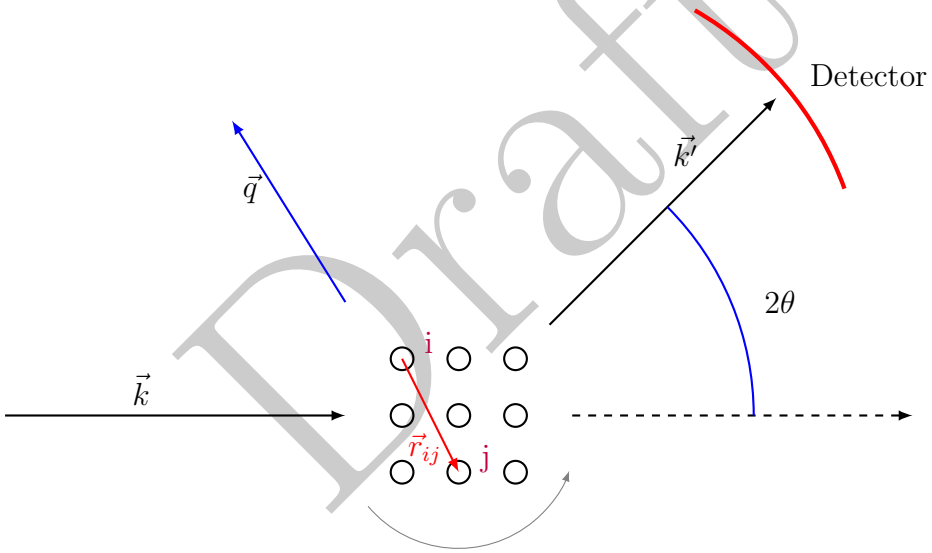

Figure 4: Diffraction from many scattering points

and interfere. The amplitude of each scattered wave is given by

$$A(\vec{k'}) = fe^{-i(\vec{k}-\vec{k'})\cdot\vec{r}} \tag{3}$$

As $\vec{q} = \left(\vec{k} - \vec{k'}\right)$

$$A(\vec{q}) = fe^{-i(\vec{q}\cdot\vec{r})} \tag{4}$$

For N scatterers we sum the waves from each scatterer j

$$A(\vec{q}) = \sum_{j=1}^{N} f_j e^{-i(\vec{q}\cdot\vec{r_j})} \tag{5}$$

The detector will measure the intensity of the radiation at each pixel summed over all scatterers. This is equal to the square of the scattering amplitude A, being a complex number - strictly the product of the amplitude with its first complex conjugate.

$$I(\vec{q}) = |A||A^*| = \sum_{j=1}^{N}\sum_{k=1}^{N} f_j f_k e^{-i\ \vec{q}\cdot\vec{r_{jk}}} \tag{6}$$

The Bragg peaks at $n\lambda = 2d\sin\theta$ give information from any long-range ordering. These simulations are concerned with short-range order resulting from the growth of crystal domains. The size of domains may be inferred from the broadening of the Bragg peaks using the Scherrer equation [1]

$$\tau = \frac{K\lambda}{\beta\sin\theta} \tag{7}$$

where τ is the domain size, K a dimensionless shape parameter generally taken as 0.9. β is the full width - half maximum peak broadening expressed in radians and θ the Bragg angle.

1.4. The Role of Reciprocal Space

Reciprocal space (also known as *momentum space or k-space*) is is a convenient abstraction when considering diffraction from a periodic structure being the Fourier transform of the real space *direct* lattice. Points in reciprocal space represent families of planes in the direct lattice, see fig 5. A key feature is that the vector direction between any two point in the reciprocal lattice represents the direction between two planes in the direct lattice and the spacing between points in k-space is the reciprocal of the inter-planar spacing. Expressing these reciprocal lattice vector lengths as $|\vec{G}| = \frac{2\pi}{\lambda}$ gives the distance in radians per unit length.

If we have a set of atomic positions in real space $\vec{r_i} = (h\vec{x_i} + k\vec{y_i} + l\vec{z_i})$ then the Fourier transform is given by

$$f(\vec{r}) = \sum_{G} f(\vec{G}) e^{i(\vec{G}\cdot\vec{r})} \tag{8}$$

The key point here is that this transform maps directly the diffraction pattern from the scatterers i.e.

$$S(\vec{q}) = \sum_{i,j,k} e^{i\vec{G}\cdot\vec{r}} \tag{9}$$

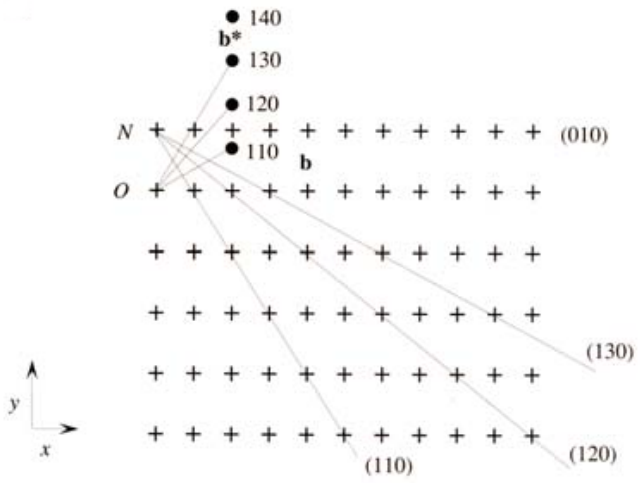

Figure 5: Construction of the Reciprocal Lattice.

Real space points are +, reciprocal points •

The reciprocal lattice axis vectors are given by

$$\vec{b}_1 = 2\pi\frac{\vec{a}_2 \times \vec{a}_3}{\vec{a}_1 \cdot \vec{a}_2 \times \vec{a}_3} \qquad \vec{b}_2 = 2\pi\frac{\vec{a}_3 \times \vec{a}_1}{\vec{a}_1 \cdot \vec{a}_2 \times \vec{a}_3} \qquad \vec{b}_3 = 2\pi\frac{\vec{a}_1 \times \vec{a}_2}{\vec{a}_1 \cdot \vec{a}_2 \times \vec{a}_3} \quad (10)$$

Note that $\vec{b}_1$ is orthogonal to both $\vec{a}_2$ and $\vec{a}_3$, $\vec{b}_2$ is to both $\vec{a}_1$ and $\vec{a}_3$ and so on. Points in the reciprocal lattice are mapped as

$$\vec{G} = h\vec{b}_1 + k\vec{b}_2 + l\vec{b}_3 \quad (11)$$

As is generally accepted, diffraction peaks occur when $\vec{q} = \vec{G}$. [2]

2. Simulating a Diffraction Pattern

Given a known crystal structure one may calculate the reflections from specific planes - the inverse of conventional experimental crystallography. This however assumes both explicit knowledge of the crystal structure and a near infinite lattice. What if one has neither. Possibly after modelled ordering via some sort of simulation and that the ordering is short-range and/or faint and one cannot be sure of the structure. A virtual diffraction image may help discern the nature of any ordering.

The alternative approach, used here is to calculate the diffraction pattern from a set of atomic positions mirroring the physical processes in experimental

x-ray or neutron crystallography. Such an *a priori* technique makes few of the assumptions of conventional crystallography such as 'reflection from planes' though is computationally somewhat expensive. Since we are considering an *a priori* algorithm it may be helpful to initially limit standard crystallographic terminology and formulate the problem in general physical terms.

- We wish to simulate the diffraction pattern formed when a beam of radiation is incident upon a group of atoms.
- These scatterers interact with the incident radiation resonating and emitting a spherical wavefront.
- Different elements will have different scattering powers.

A number of methods have been developed to simulate diffraction patterns directly from atomistic data.

2.1. Direct Scattering Simulation

The most direct method takes a rather *brute force* approach. One simply determines the linear path lengths, L_i from a monochromatic coherent radiation source to each atom in the model and from there to every pixel on the detector array . Sin and cos of $2\pi\frac{L_i}{\lambda}$ for each path are summed at each pixel giving the resultant amplitude and phase. This scales directly with $N_{atoms} \times n_{pixels}$ for a sample of 10^6 atoms and a linear detector of 10^4 pixels one has of the order of 10^{10} iterations - perfectly acceptable on a modern workstation. Since each calculation does not depend on the others then this is easily optimised by parallel processing. One problem here though is the need for the path lengths to be very long compared to the size of the sample and hence the differences in atomic positions. This is to avoid distortion of the pattern by some parts of the sample being significantly closer to the detector than others. If the simulation mirrors a real diffractometer the sample $\rightarrow$ detector distance will be $> 10^8\times$ the inter-atomic spacing. Assuming that we need to resolve path differences of 10^{-2} of this spacing we require a precision of $1 : 10^{10}$. To overcome this one needs to use high precision 'long' real numbers which significantly slows the computation.

2.2. Using Pairwise Distributions

A more sophisticated approach involves calculating

$$I(\vec{k'}) = \sum_{i \neq j} \sum_{j} e^{i\vec{q}\cdot\vec{r}_{ij}} \tag{12}$$

to every point on the detector array see fig 4. If we assume that, to the incoming radiation, each atom acts as a point scatterer and that the atoms do not move their positions may be represented as a series of δ-functions. A further simplification may be introduced by assuming that the size of the region being sampled is much smaller than the distance between the sample and the detector. Thus we can assume that the scattering distance and angle from each atom to each point on the detector are approximately constant. The problem with this method is again the computational load. For a sample of 10^5 atoms and a 2d detector of 10^6 pixels one would need to perform some 10^{16} calculations before needing to rotate the sample to ensure that all possible peaks are detected. Without some optimisation of the algorithm this is impractical. This has the appearance of Fourier transform and so it should be practical to perform an F.F.T. if we assume that the scatterers are both point entities and sit on points fixed on a regular 3d lattice. If the points are permitted to displace from these regular points, via thermal vibration or during diffusion one cannot perform an FFT. This could be addressed by defining a grid whose spacing is much smaller than the lattice parameter and limiting scatters to these discrete positions. With say 10^6 atoms and 10 intermediate points between the *regular* lattice sites results in a grid of 10^9 points with only 0.1% filled at any time. This will lead to very large data-arrays which without some optimisation will again add to the computation time.

2.3. Pair Distribution Functions (PDF)

The diffraction pattern is a function of the degree of spatial ordering within the sample and therefore of the density distribution of scatterers. Taking into account such a pair distributions is of particular importance when considering partly ordered systems. S The reduced pair distribution function – $g(r)$ is simply the probability of finding a pair of particles at a specific distance r from one another. $g(r)$ is often expressed in the normalised form such that as $r \to \infty, g(r) \to 1$ and for $r <$ distance of closest approach $g(r) = 0$. The pair distribution function may be obtained directly from a molecular dynamics simulation where it is related to the pair density function $\rho(r)$ by $\rho(r) = \rho_0 g(r)$. As $r \to \infty$, $\rho(r)$ will tend to ρ_0, the mean number density of the sample and tend to zero as $r \to 0$

$$g(r) = 4\pi r \left(\rho(r) - \rho_0\right) = 4\pi\rho_0 r \left(g(r) - 1\right) \tag{13}$$

Within a shell at a range $r_1 \to r_2$ we may specify the number of neighbours,

a site's coordination number as

$$N_c = \int_{r_1}^{r_2} R\,(r)\,dr \tag{14}$$

In the Debye-Glatter scattering method [3] rather than performing the computationally intensive *sin* calculation for every atom pair the calculation is optimised 'binning' these coordination numbers, see fig 6, in advance then calculating

$$I(q) = \frac{1}{N}\sum_{i=1}^{N} f_i N_{c_i} \frac{sin(2\pi q r_i)}{2\pi q r_i} \tag{15}$$

i.e. The inter-atomic distances are calculated for every atom-atom pair then divided into a histogram where the width of each 'bin' is suitably small to give the desired resolution. The double summation over all atomic pairs is thus reduced to a single sum over N bins.

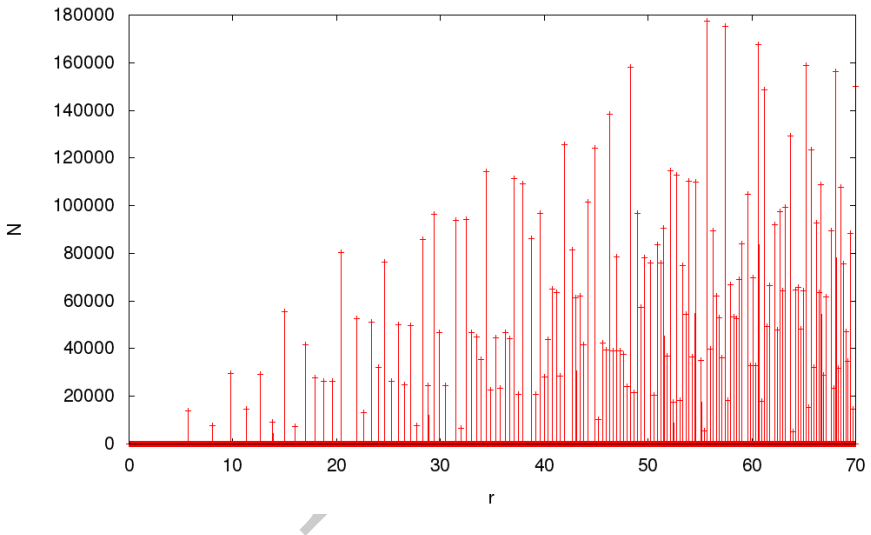

Figure 6: Example of binned interatomic distances for C=0.29 ordered f.c.c. lattice

We may now specify a radial distribution function $R(r)$ describing the number of atoms in a shell of thickness $d(r)$ at a distance r:-

$$R(r) = 4\pi r^2 \rho(r) \tag{16}$$

giving

$$g(r) = \frac{R(r)}{r} - 4\pi r \rho_0 \tag{17}$$

This may be easily determined at any point in a molecular dynamics simulation. If we assume initially that atoms sit at precise positions $\vec{r_i}$ without thermal or other displacements then their positions may be expressed as a series of delta functions $\delta\left(\vec{r_0} - \vec{r_i}\right)$. Setting $\vec{r_0} = 0$ gives

$$R(r) = \frac{1}{N} \sum_i \sum_j \delta\left(\vec{r_{ij}}\right) \tag{18}$$

The reduced pair distribution function $g(r)$ is the Fourier Transform of $S(q)$ the total scattering structure function – effectively the normalised diffraction intensity.

$$G(r) = \frac{2}{\pi} \int_{qmin}^{qmax} q[S(q) - 1] sin(qr) dq \tag{19}$$

The inverse transform is more useful here

$$S(q) = 1 + \frac{1}{q} \int_0^{\infty} r(r) sin(qr) dr \tag{20}$$

In the 1980s a simulation technique using the Debye scattering equation for powder samples was developed [3].

$$I(q) = \frac{1}{N} \sum_{i=1}^{N} \sum_{j=1}^{N} f_i f_j \frac{sin(2\pi q r_{ij})}{2\pi q r_{ij}} \tag{21}$$

where f_i, f_j are the scattering factors of the respective atoms and q, r_{ij} are equal to $|\vec{q}|$ and $|\vec{r_{ij}}|$ respectively. S

The algorithm may be optimised by binning the distances r_{ij} before performing the computationally intensive *sin* calculations. With sufficiently narrow bins the errors generated are minimal, see fig 6. In effect this technique loses the absolute spatial, i.e. directional, information in favour of a computationally faster method of generating pair distributions (the bins). The size of crystal regions may be inferred from peak broadening rather than being directly observed. This technique is very fast, on a 3 GHz workstation a pattern from 10^4 atoms, with 10^4 detector pixels and 10^5 bins computes in some 100 seconds, see fig 7. Scaling to a more realistic 10^6 atoms takes $\sim$ 3 hours.

The technique used here for the contour 2d plots involves summing $e^{i\left(\vec{G}\cdot\vec{r_i}\right)}$ over a range of G_x and G_y see fig 8.

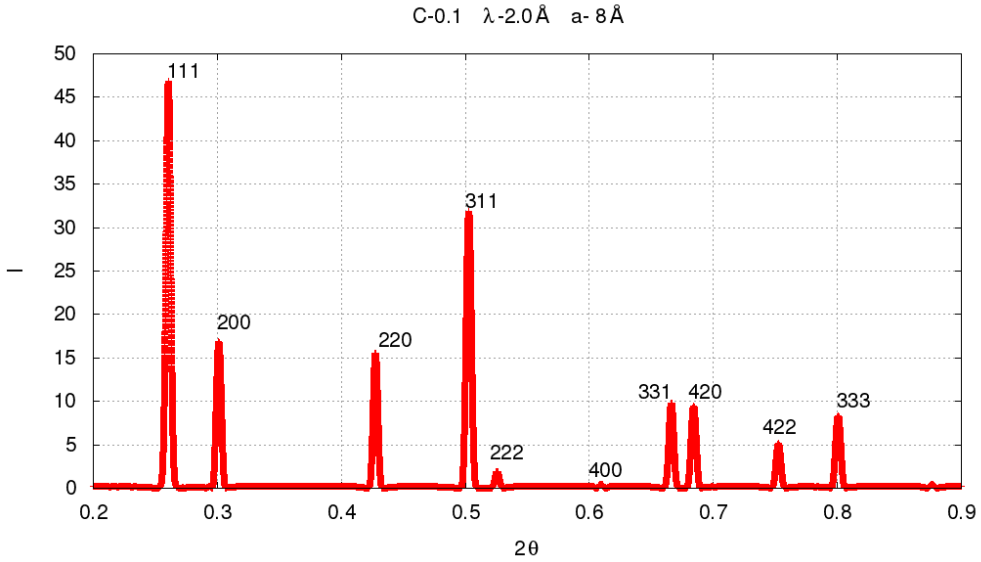

Figure 7: Virtual Debye Diffraction Pattern of H in Pd demonstrating hkl all odd or all even as expected for f.c.c. structure

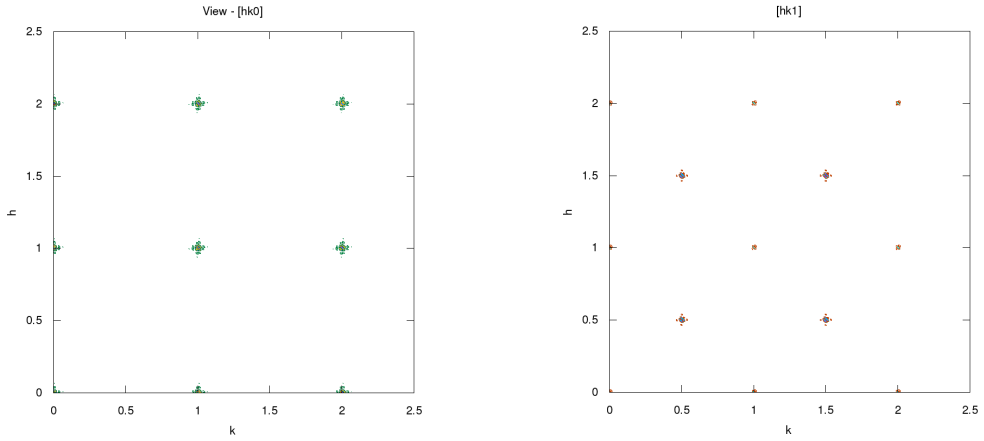

Figure 8: Sample 2d contour plots of partly filled f.c.c. *(f.c.c. real space → b.c.c reciprocal space)* lattice in hk0 and hk1

3. Symbols

A	scattered amplitude
f	atomic scattering factor
$\vec{k}$	incident wave vector
$\vec{k'}$	scattered wave vector
$\vec{q}$	diffraction vector
R_j	distance from j^{th} atom to detector
$\vec{r_{ij}}$	displacement vector between i^{th} andj^{th} atoms
τ	domain size
θ	Bragg Angle
K	shape parameter in Scherrer equation
β	full width - half maximum peak broadening
$\vec{G}$	reciprocal lattice vector

4. References

[1] A. L. Patterson, "The scherrer formula for x-ray particle size determination," *Phys. Rev.*, vol. 56, pp. 978–982, Nov 1939.
[2] C. Kittel, *Introduction to Solid State Physic 8th Edition*. Wiley, 2005.
[3] O. Glatter and O. Kratky, *Small angle X-ray scattering*. London: Academic Press Inc, 1982.